IgG1 B cell receptor signaling is inhibited by CD22 and promotes the development of B cells whose survival is less dependent on Igα/β

Ari Waisman,[1] Manfred Kraus,[1,4,5] Jane Seagal,[4,5] Snigdha Ghosh,[6] Doron Melamed,[4,5,7] Jian Song,[1,2,3] Yoshiteru Sasaki,[4,5] Sabine Classen,[1] Claudia Lutz,[8] Frank Brombacher,[9] Lars Nitschke,[6] and Klaus Rajewsky[1,4,5]

[1]Institute for Genetics and [2]Center for Molecular Medicine, University of Cologne, 50674 Cologne, Germany
[3]I. Medical Department, Johannes Gutenberg-University Mainz, 55131 Mainz, Germany
[4]CBR Institute for Biomedical Research and [5]Department of Pathology, Harvard Medical School, Boston, MA 02115
[6]Department of Genetics, University of Erlangen, 91058 Erlangen, Germany
[7]Department of Immunology, Ruth and Bruce Rappaport Faculty of Medicine and Rappaport Family Institute for Research in the Medical Sciences, Technion-Israel Institute of Technology, Haifa 31096, Israel
[8]Max-Planck-Institute of Immunobiology, 79011 Freiburg, Germany
[9]Department of Immunology, Groote Schuur Hospital, University of Cape Town, Cape Town 7925, South Africa

The Journal of Experimental Medicine

We describe a mouse strain in which B cell development relies either on the expression of membrane-bound immunoglobulin (Ig) γ1 or μ heavy chains. Progenitor cells expressing γ1 chains from the beginning generate a peripheral B cell compartment of normal size with all subsets, but a partial block is seen at the pro– to pre–B cell transition. Accordingly, γ1-driven B cell development is disfavored in competition with developing B cells expressing a wild-type (WT) IgH locus. However, the mutant B cells display a long half-life and accumulate in the mature B cell compartment, and even though partial truncation of the Igα cytoplasmic tail compromises their development, it does not affect their maintenance, as it does in WT cells. IgG1-expressing B cells showed an enhanced Ca^{2+} response upon B cell receptor cross-linking, which was not due to a lack of inhibition by CD22. The enhanced Ca^{2+} response was also observed in mature B cells that had been switched from IgM to IgG1 expression in vivo. Collectively, these results suggest that the γ1 chain can exert a unique signaling function that can partially replace that of the Igα/β heterodimer in B cell maintenance and may contribute to memory B cell physiology.

CORRESPONDENCE
Klaus Rajewsky
rajewsky@cbr.med.harvard.edu
OR
Ari Waisman:
waisman@uni-mainz.de

Abbreviations used: BAFF, B cell–activating factor; BCR, B cell receptor; C, constant region; CFSE, carboxyfluorescein succinimidyl ester; ERK, extracellular signal–related kinase; ES, embryonic stem; H, heavy; HRP, horseradish peroxidase; JNK, c-Jun N-terminal kinase; MZ, marginal zone; pBCR, pre-BCR; SHP-1, Src homology domain 2–containing protein tyrosine phosphatase; TLR, Toll-like receptor.

Although Ig heavy (H) chains of the classes α, ε, and γ carry evolutionarily conserved cytoplasmic tails of 14–28 amino acids, such structures are essentially lacking in μ and δ chains (1–3). As the latter are expressed in developing and mature naive B cells, the signaling function of the B cell receptor (BCR) on those cells is thought to rely entirely on the cytoplasmic tails of the BCR-associated Igα/β heterodimer. However, in the generation of B cell memory, most of the antigen-activated B cells participating in the response switch to the expression of other antibody isotypes, and the BCRs on these cells acquire the cytoplasmic tail of the newly expressed IgH chain as an additional signaling module. Although the distinct transmembrane domains of the newly expressed IgH chains may also contribute to signaling, the functional importance of the γ1 and ε cytoplasmic tails became apparent in experiments in which the gene segments encoding these structures, respectively, were deleted in the mouse germ line, and a profound deficiency in the development of IgG1- or IgE-expressing memory B cells was observed (4,5). These results were complemented and extended by a study in which transgenic expression of γ1 or μ/γ hybrid chains conferring a particular antigenic specificity in combination with a transgenic κ light chain led to an enhanced generation of memory and plasma

A. Waisman, M. Kraus, J. Seagal, L. Nitschke, and K. Rajewsky contributed equally to this work.
M. Kraus's present address is Merck Research Laboratories, Boston, MA 02115.
The online version of this article contains supplemental material.

Table I. B cell populations in the BM

Genotype	No.	Percentage of all BM cells			
		Pro-B (A–C)	Pre-B (D)	Immature (E)	Recirculating (F)
$IgH^{+/+}$ $Ig\alpha^{+/+}$	$n = 6$	2.8 ± 0.9	14.8 ± 6.3	7.8 ± 1.5	3.3 ± 0.5
$IgH^{\gamma1\mu/\gamma1\mu}$ $Ig\alpha^{+/+}$	$n = 6$	6.4 ± 2	8.4 ± 5.2	5.1 ± 3.9	4.6 ± 1.9
$IgH^{\gamma1\mu/\gamma1\mu}$; $Ig\alpha^{\Delta c1/\Delta c1}$	$n = 5$	4 ± 2.3	5.3 ± 2.1	0.83 ± 0.48	0.61 ± 0.37
$IgH^{+/+}$ $Ig\alpha^{\Delta c1/\Delta c1}$	$n = 5$	6.1 ± 3.6	1.1 ± 0.7	0.59 ± 0.4	0.07 ± 0.06

Values represent the mean ± SD.

cell progeny upon antigenic challenge because of reduced cellular attrition (6). The molecular basis of these effects has not been elucidated, except by a provocative study suggesting that the γ2a cytoplasmic tail enhances BCR signaling by preventing immunoreceptor tyrosine–based inhibition motif phophorylation of the inhibitory CD22 coreceptor (7).

The conspicuous absence of cytoplasmic tails in μ and δ chains could reflect peculiar signaling requirements in pre–B and immature B cells, predicting that expression of IgH chains with cytoplasmic tails would compromise B cell development. Indeed, although δ chains alone can efficiently mediate B cell development (8, 9), transgenic expression of γ chains of various classes often seemed to disturb normal development (10–15), sometimes promoting the generation of cells coexpressing endogenous μ and δ chains (16–20). However, the physiological significance of these experiments remained uncertain given the variations in transgene copy number and, consequently, expression levels inherent in the experimental approach. In this paper, we address this question, as well as that of the physiological role of γ1 chain–containing BCRs in general, in a new experimental setting by replacing the constant region (C) gene cluster in the IgH locus (C_H) with a loxP-flanked simplified locus containing a Cμ and a Cγ1 gene segment in opposite orientation in mouse embryonic stem (ES) cells, allowing the derivation of mutant strains that exclusively express either membrane-bound IgM or IgG1 in the B cell lineage. It is also possible in these mice to switch B cells in the mutant animals from IgM to IgG1 expression, or vice versa, in a Cre recombinase–dependent manner.

RESULTS

Construction of a mutant IgH locus from which either IgM or IgG1 can be expressed exclusively in a Cre recombinase–dependent manner

Starting from ES cells in which the Cδ gene segment replaced that of Cμ (9), we constructed an IgH locus whose C gene cluster was modified to contain only the Cμ and Cγ1 gene segments (Fig. S1, available at http://www.jem.org/cgi/content/full/jem.20062024/DC1). These gene segments were organized in opposite orientations. The new minilocus, which was successfully transmitted into the germ line, was flanked by loxP sites in opposite orientations, such that Cre-mediated recombination would either switch B cells in vivo from IgM to IgG1 expression (or vice versa) or, when induced in the germ line, generate strains of mice exclusively expressing either IgM or IgG1 in the B cell lineage. As our original intention was to compare IgM- and IgG-mediated antigen presentation by B cells, we deleted the polyA sites controlling the production of the secreted forms of the μ and γ1 chains, respectively. Depending on the C_H gene segment in the upstream position, the mutant IgH loci were designated $IgH^{\mu\gamma1}$ or $IgH^{\gamma1\mu}$. As expected, homozygous $IgH^{\mu\gamma1}$ mice produced a B cell compartment consisting exclusively of B cells expressing the membrane form of IgM, with no IgM being detectable in the blood (unpublished data). In contrast, homozygous $IgH^{\gamma1\mu}$ mice exclusively produced IgG1-expressing B cells, as further described below. However, contrary to our expectation, large amounts of IgG1 were detectable in the blood of these animals, presumably because of the usage of

Table II. B cell populations in the spleen

Genotype	No.	T cells ($\times 10^6$)	B cells ($\times 10^6$)	Transitional $AA4.1^+$ cells (% of B cells)	T1 cells (% of $AA4.1^+$ cells)	B1 cells (% of B cells)	B1 cells ($\times 10^6$)	MZ cells (% of B cells)	$\lambda1^+$ cells (% of B cells)
$IgH^{+/+}$ $Ig\alpha^{+/+}$	$n = 7$-10	24.7 ± 9	29.1 ± 7.6	18.6 ± 3.1	55.4 ± 6.2	3.03 ± 0.25	0.97 ± 0.28	7.2 ± 1.2	4 ± 0.8
$IgH^{\gamma1\mu/\gamma1\mu}$ $Ig\alpha^{+/+}$	$n = 7$-10	28.7 ± 6.6	33.1 ± 13.1	15.5 ± 10	38 ± 4.8	0.96 ± 0.27	0.26 ± 0.11	15 ± 3.5	9.7 ± 0.8
$IgH^{\gamma1\mu/\gamma1\mu}$; $Ig\alpha^{\Delta c1/\Delta c1}$	$n = 4$-8	20.5 ± 6.8	3.7 ± 2	6.6 ± 2.3	58.2 ± 7.8	12.4 ± 3.8	0.37 ± 0.19	7.1 ± 2.4	12.8 ± 2.3
$IgH^{+/+}$ $Ig\alpha^{\Delta c1/\Delta c1}$	$n = 4$	11.7 ± 2.6	0.3 ± 0.3	ND	ND	ND	ND	ND	ND

Values represent the mean ± SD.

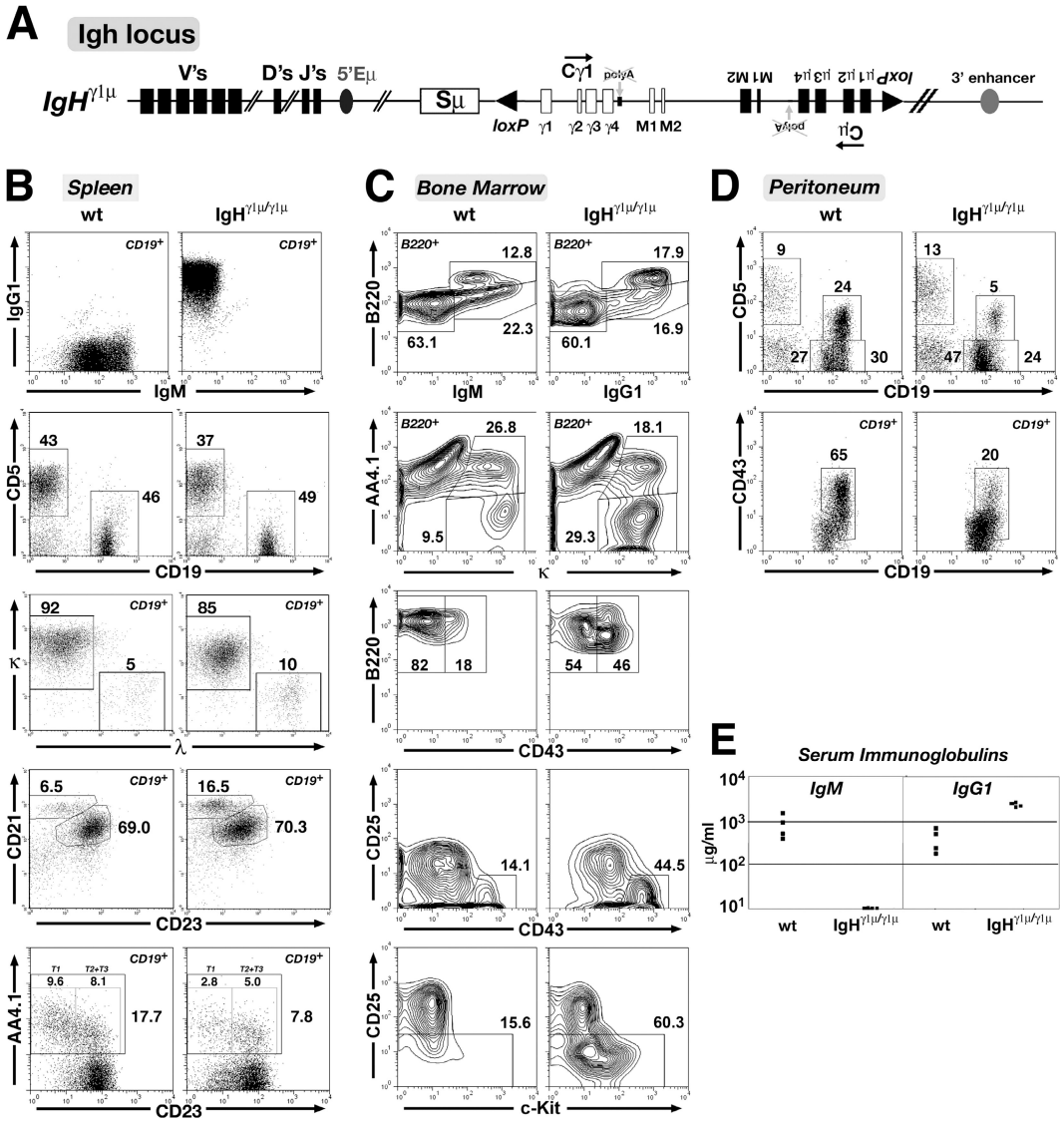

Figure 1. The γ1 H chain supports B cell development in IgH$^{\gamma1\mu/\gamma1\mu}$ mice. (A) Genomic structure of the IgH$^{\gamma1\mu}$ locus. To generate the IgH$^{\gamma1\mu}$ allele, all C_H regions of the IgH locus were replaced by the Cγ1 region, followed by the Cμ region in opposite transcriptional orientation, flanked by inverted loxP sites (triangles). Inversion of the loxP-flanked region by Cre recombinase generates B cells that exclusively express γ1 (IgH$^{\gamma1\mu}$) or μ (IgH$^{\mu\gamma1}$; not depicted). (B) Flow cytometric analysis of splenocytes from IgH$^{\gamma1\mu/\gamma1\mu}$ mice. Expression of membrane IgG1 and IgM by CD19$^+$ B cells is shown (top). Splenocytes were stained for CD5 and CD19 expression to estimate the ratio between T cells and B cells (second panel from the top). The ratio of κ/λ light chain usage in splenic CD19$^+$ B cells is shown (third panel from the top). The ratio of MZ B cells (CD19$^+$CD21^{bright}CD23$^-$) and follicular B cells (CD19$^+$CD21$^+$CD23^{bright}) is shown (fourth panel from the top). Transitional B cell fractions were determined by AA4.1 and CD23 expression levels (gated on B220$^+$ cells; bottom). Numbers represent the percentage of cells within the designated gates. (C) In the two top panels, B cell development in the BM of IgH$^{\gamma1\mu/\gamma1\mu}$ mice. B220$^+$ B lymphocytes are displayed and gated based on expression levels of surface Ig, B220, and the maturation marker AA4.1 to determine the immature (B220^{lo}Ig$^+$AA4.1$^+$; fraction E) and mature (B220^{hi}Ig$^+$AA4.1$^-$; fraction F) fractions (reference 38). The three bottom panels show the distribution of pro–B cell (CD43$^+$CD25$^-$; fractions A–C) versus pre–B cell (CD43$^-$CD25$^+$; fraction D) populations within B220$^+$Ig$^-$-gated BM cells. Numbers represent the percentage of cells within the designated gates. (D) Flow cytometric analysis of peritoneal cells in IgH$^{\gamma1\mu/\gamma1\mu}$ mice. (top) Dot plots show the percentages of cells within the lymphocyte gate: T cells (CD5^{high}CD19$^-$), B-1a cells (CD19^{high}CD5$^+$), B-1b cells (CD19^{high}CD5^{low}), and B-2 cells (CD19^{lwo}CD5^{low}). (bottom) The fraction of CD43$^+$CD19^{hi} cells within the CD19$^+$ peritoneal B lymphocytes. (E) IgM and IgG1 titers in the sera of IgH$^{\gamma1\mu/\gamma1\mu}$ mice. Ig levels were determined by ELISA. Each dot represents values obtained from an individual mouse.

Table III. B cell populations in the peritoneal cavity

Genotype	No.	B cells	B1a	B1b	B2
		% of all cells	% of B cells		
$IgH^{+/+}$ $Ig\alpha^{+/+}$	$n = 6$	72 ± 9	29 ± 13.5	36.8 ± 7	33.8 ± 9.8
$IgH^{\gamma1\mu/\gamma1\mu}$ $Ig\alpha^{+/+}$	$n = 6$	74 ± 8	6.5 ± 4.6	32.7 ± 7	60.6 ± 8.9
$IgH^{\gamma1\mu/\gamma1\mu}$; $Ig\alpha^{\Delta c1/\Delta c1}$	$n = 5$	12 ± 6	37.9 ± 16.4	50.9 ± 14.8	10.9 ± 5
$IgH^{+/+}$ $Ig\alpha^{\Delta c1/\Delta c1}$	$n = 3$	3 ± 1	9.5 ± 5.3	45.6 ± 19.2	44.8 ± 13.9

Values represent the mean ± SD.

an alternative polyA site (Fig. 1 E). B cell development and maintenance in this latter mouse strain is the subject of this study.

γ1 chains mediate the generation of mature B cells of all subsets

The $IgH^{\gamma1\mu}$ locus is schematically depicted in Fig. 1 A, and the populations of B lineage cells in the spleen, BM, and peritoneal cavity of homozygous $IgH^{\gamma1\mu}$ mice are depicted in Fig. 1 (B–D). A survey of the composition of the various B cell compartments in mutant and control animals is given in Tables I–III. In the spleens of adult mutant mice, transitional, mature B2, and marginal zone (MZ) B cells could be detected on the basis of expression of typical surface markers, and all B cells expressed IgG1 instead of IgM on the surface. In comparison to the controls, the absolute numbers of splenic B cells were normal, but we found a reduction in the fractions of transitional, in particular T1, cells and a two- to threefold increase in the fraction of MZ B cells (Fig. 1 B and Table II). These deviations from the normal situation indicated an impairment of B cell development in the mutant animals that became more apparent when B cell development in the BM was analyzed by flow cytometry. Staining of the cells for B220, c-Kit, CD43, and CD25 revealed a partial block at the pro– to pre–B cell transition (Fig. 1 C and Table I). Accordingly, although the total cell numbers in the BM of $IgH^{\gamma1\mu/\gamma1\mu}$ and WT mice were comparable (11.9 ± 1.7 and 11.4 ± 1.6 million cells per femur, respectively), the numbers of immature B cells in the BM and the spleen, identified by low levels of B220 and high levels of AA4.1, respectively, were also somewhat reduced in the mutant animals in comparison with the controls (Fig. 1, B and C; and Tables I and II).

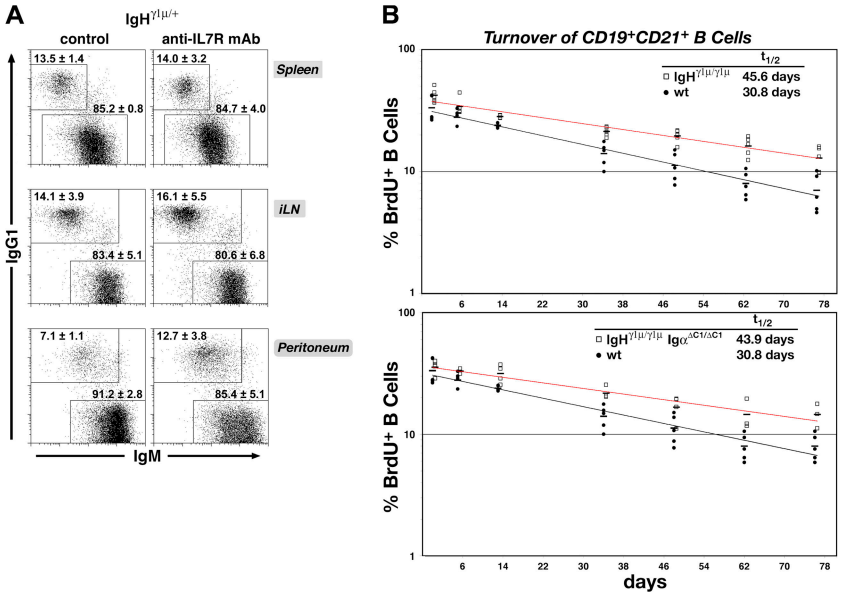

Figure 2. IgG1⁺ B cells are underrepresented in heterozygous $IgH^{\gamma1\mu/+}$ mice because of impaired early B cell development rather than a reduced life span. (A) IgM^+ and $IgG1^+$ fractions of $CD19^+$ B cells from spleen, inguinal lymph nodes, and the peritoneal cavity. (right) Dot plots represent mice that were treated for 30 d with an IL-7 receptor antibody to block the influx of newly generated B cells from the BM. Controls were injected with PBS. The blocking of B cell development in mice treated with IL-7 receptor antibody was confirmed by flow cytometric analysis of the BM cells (not depicted). Numbers represent the percentage (mean ± SD) calculated from two experiments with a total of eight mice. (B) Life spans of B cells in $IgH^{\gamma1\mu/\gamma1\mu}$ and $IgH^{\gamma1\mu/\gamma1\mu}$ $Ig\alpha^{\Delta c1/\Delta c1}$ mice. After a labeling period of 1 mo, BrdU incorporation in mature peripheral blood B lymphocytes ($CD19^+CD21^+$) was measured at the indicated time points (day 0 = beginning of chase period). Each symbol represents an individual mouse, and the horizontal lines represent the mean. Calculated decay curves and half-lives are shown.

Table IV. Survival advantage of IgG1$^+$ cells over IgM$^+$ competitor B cells

		IgG1$^+$/IgM$^+$ ratio					
		BM		Spleen			
Genotype	No.	Immature	Mature/ recirculating	T1	T2/T3	All transitional	Mature
		AA4.1$^+$ B220$^+$	AA4.1$^-$ B220$^+$	AA4.1$^+$CD23$^-$ CD19$^+$	AA4.1$^+$CD23$^+$ CD19$^+$	AA4.1$^+$ CD19$^+$	AA4.1$^-$ CD19$^+$
IgH$^{\gamma1\mu/+}$ Igα$^{\Delta c/+}$	$n = 5$	0.06 ± 0.01	0.16 ± 0.02	0.058 ± 0.012	0.106 ± 0.007	0.08 ± 0.01	0.16 ± 0.02
IgH$^{\gamma1\mu/+}$ Igα$^{\Delta c1/\Delta c1}$	$n = 5$	0.83 ± 0.22	2.24 ± 0.71	ND	ND	2.09 ± 0.29	2.68 ± 0.3

In heterozygous IgH$^{\gamma1\mu/+}$ Igα$^{\Delta c+/+}$ and IgH$^{\gamma1\mu/+}$ Igα$^{\Delta c1/\Delta c1}$ mice, the IgG1$^+$/IgM$^+$ B cell ratio increases with the maturational status. Note the strong increase of the fraction of IgG1$^+$ B cell presence within the mature compartment. BM and splenic cells were surface stained for IgG1/IgM, AA4.1, CD23, and a B cell–specific marker (B220 or CD19) and analyzed by flow cytometry.

In the peritoneal cavity, both B1 and B2 cells were detectable in the mutants, but the fraction of B1a (CD5$^+$CD43$^+$CD19^{high}) was substantially reduced compared with the controls (Fig. 1 D).

We conclude that expression of γ1 instead of μ chains is compatible with the development of B cells of all subsets, but that the development of B1 and B2 cells is compromised.

B cells expressing Igγ1 chains compete poorly with their IgM-expressing counterparts in development but mature into long-lived, B cell–activating factor (BAFF)–dependent cells that respond to BCR and Toll-like receptor (TLR) stimulation

Heterozygous IgH$^{\gamma1\mu}$ mice allowed us to study the development of γ1 and μ/δ chain–expressing B cells in competition. As expected from the compromised development of IgG1-expressing cells (Fig. 1 C), the peripheral B cell compartment was dominated in this situation by IgM-expressing B cells by a factor of 6 in the spleen and lymph nodes and >10 in the peritoneal cavity (Fig. 2 A, left). Both IgM- and IgG1-expressing cells were long lived, but the IgG1-expressing cells persisted as well as and perhaps even slightly better than their IgM-expressing counterparts over 30 d of treatment with anti–IL-7 antibody, which blocks B cell generation in the BM (Fig. 2 A, right) (21). The longevity of the cells was also determined in IgH$^{\gamma1\mu}$ homozygous mice by measuring the decay of cells having incorporated BrdU, after a feeding period of 1 mo, over time (Fig. 2 B). Strikingly, the apparent half-life of the mutant cells, averaged over the population of CD19$^+$CD21$^+$ B cells in the blood, was longer than that of WT cells by a factor of 1.5. This difference does not necessarily indicate an intrinsic property of these cells distinguishing them from their IgM- and IgD-expressing counterparts but could simply reflect the diminished output of B cells from the BM in the mutant animals. Nevertheless, the mutant cells were clearly long-lived, and this explains how IgH$^{\gamma1\mu}$ mice can generate a peripheral B cell compartment similar in size to that of WT mice despite a defect in B cell generation. It may also explain why the apparent counterselection of the IgG1- expressing cells is stronger at the level of immature and transitional T1 cells as compared with mature B cells (Table IV).

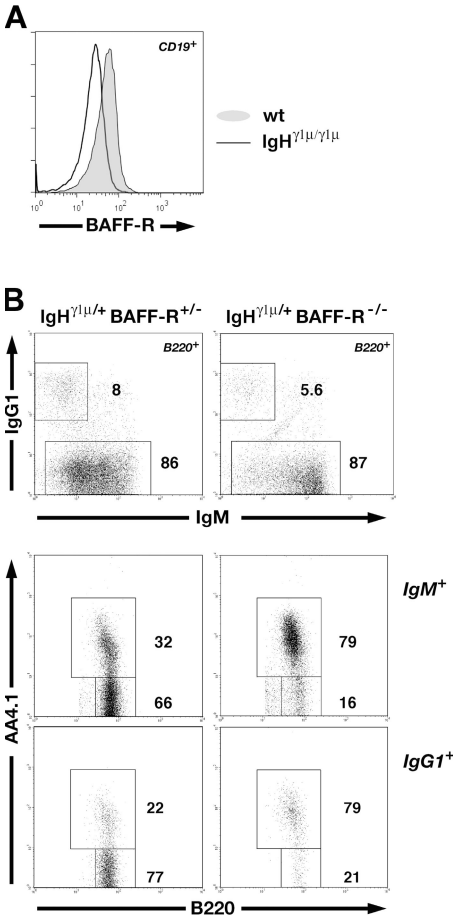

Figure 3. BAFF-R dependence of IgG1$^+$ B cells. (A) BAFF-R expression levels in CD19$^+$ splenic B cells. (B) Flow cytometric analysis of splenic B cells from IgH$^{\gamma1\mu/+}$ BAFF-R$^{-/-}$ mice. IgG1$^+$ B cells depend on BAFF-R for maintenance. (top) B220$^+$ B cells from IgH$^{\gamma1\mu/+}$ BAFF-R$^{-/-}$ mice and IgH$^{\gamma1\mu/+}$ BAFF-R$^{-/+}$ controls. (bottom) The IgM$^+$ and IgG1$^+$ B cell fractions from the top panel are further analyzed for their mature (AA4.1$^-$) versus immature (AA4.1$^+$) composition. Numbers represent the percentage of cells within the designated gates.

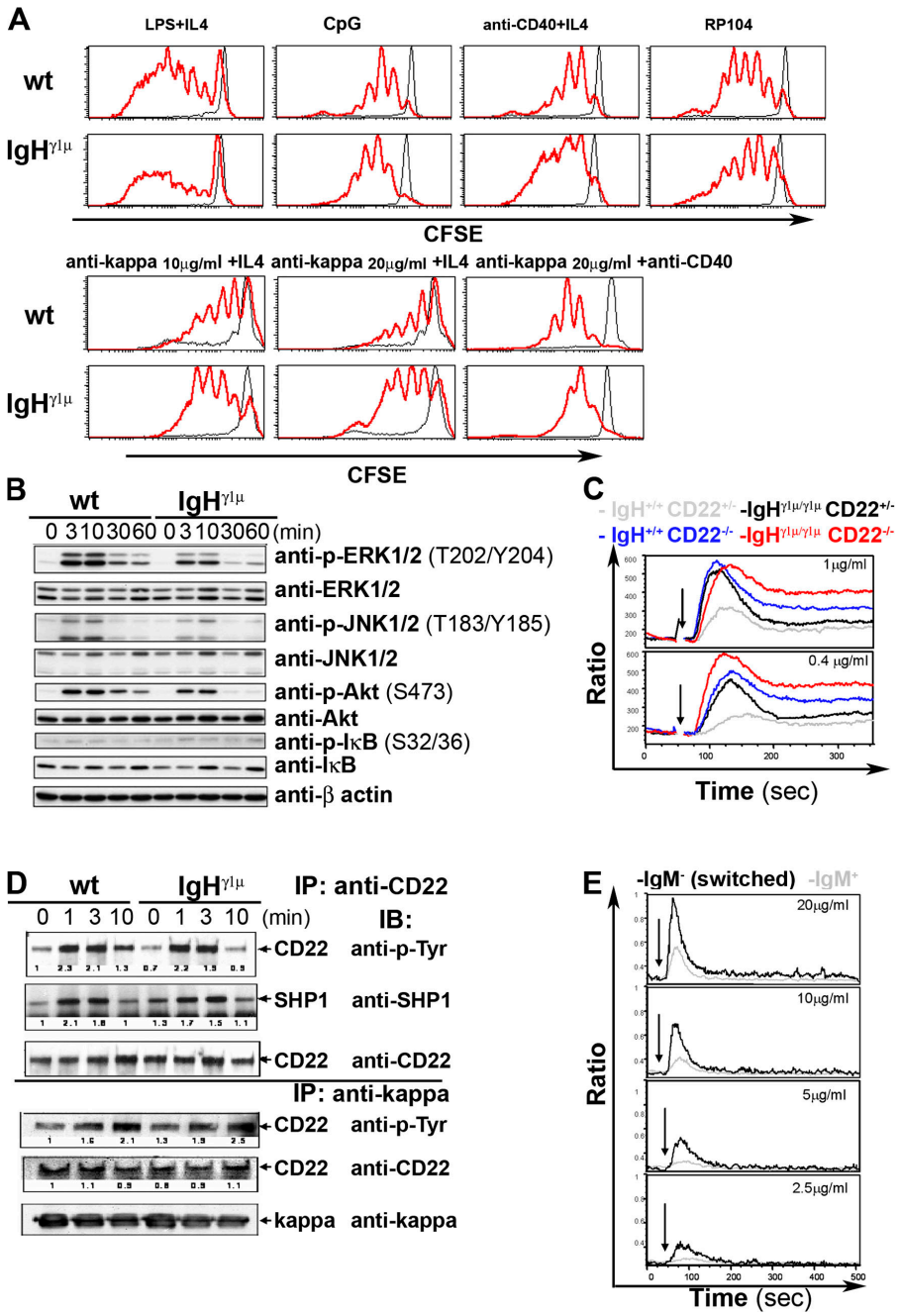

Figure 4. IgG1$^+$ B cells show enhanced proliferative and Ca^{2+} responses, which are not caused by a lack of CD22 inhibition, upon BCR cross-linking. (A) Proliferative responses of IgH$^{\gamma1\mu/\gamma1\mu}$ B cells. Spleen cells from WT and IgH$^{\gamma1\mu/\gamma1\mu}$ mice were labeled with CFSE, stimulated with the indicated mitogenes, and analyzed by flow cytometry 4 d later. Histograms display CFSE fluorescence of B220$^+$ B cells. A representative analysis of four independent experiments is shown. (B) Immunoblotting for BCR-induced JNK, ERK, Akt, and IκBα phosphorylation. Splenic follicular B cells (B220$^+$CD21$^+$CD23^{bright}) from WT and IgH$^{\gamma1\mu/\gamma1\mu}$ mice were sorted with a FACSVantage and stimulated with 20 μg/ml anti-kappa for the indicated times. Whole-cell lysates were separated by SDS-PAGE and immunoblotted with the indicated antibodies. β-actin levels are shown as a loading control. (C) Ca^{2+} responses of IgH$^{\gamma1\mu}$ B cells upon BCR cross-linking in the absence and presence of CD22. Indo-1–loaded splenocytes were stimulated with 1 or 0.4 μg/ml anti-kappa at the time points indicated by the arrows. Histograms show Ca^{2+} B cell responses (CD5$^-$ Mac-1$^-$), displayed as the means of the 405/485-nm emission ratio over time. (D) Immunoprecipitation of CD22 and the BCR complex from IgH$^{\gamma1\mu/\gamma1\mu}$ splenic B cells. Splenic B cells from WT and IgH$^{\gamma1\mu/\gamma1\mu}$ mice were stimulated with 10 μg/ml anti-kappa for the indicated times, and CD22 was immunoprecipitated from the lysates. Coprecipitated proteins were detected with antiphosphotyrosine (anti–p-Tyr), anti–SHP-1, and anti-CD22. Numbers indicate the fold increase in phosphorylation of CD22 and the amount of SHP-1 precipitated compared with unstimulated WT samples, normalized to total CD22. Additionally, five experiments were analyzed, and means and SDs were calculated. The results were in the same order as in the figure: anti–p-Tyr (control), 1, 2.3 ± 0.1, 1.7 ± 0.5, and 0.8 ± 0.1; IgH$^{\gamma1\mu/\gamma1\mu}$ mice, 0.8 ± 0.1, 2.2 ± 0.1, 1.7 ± 0.3, and 1.2 ± 0.2; anti–SHP-1

Like mature IgM- and IgD-expressing B cells, the mature IgG1-expressing B cells in heterozygous $IgH^{\gamma1\mu}$ mice were dependent on BAFF–BAFF-R interaction, as shown by the loss of mature ($B220^{+}AA4.1^{-}$), but not transitional ($B220^{+}AA4.1^{+}$), splenic B cells in $IgH^{\gamma1\mu/\gamma1\mu}$ and WT mice on a BAFF-R–deficient background (Fig. 3 B). Interestingly, the IgG1-expressing B cells in homozygous $IgH^{\gamma1\mu}$ mice expressed lower levels of BAFF-R than WT B cells (Fig. 3 A), supporting the notion that there is a link between BCR signaling and BAFF-R expression (22).

The B cells of the mutant animals responded vigorously to mitogenic stimuli addressing TLRs or the BCR by proliferation. Although the proliferative responses of the IgG1-expressing B cells through TLRs and CD40 ligation were not notably different from those of control B cells, we observed a distinctly enhanced fraction of highly proliferating mutant cells upon BCR cross-linking (Fig. 4 A). These differences were more pronounced when low doses (1–10 μg/ml) of the cross-linking anti-kappa antibody were used (Fig. 4 A and not depicted).

B cells of $IgH^{\gamma1\mu}$ mice show enhanced BCR-triggered Ca^{2+} responses, which are not caused by uncoupling from CD22-mediated inhibition

Although IgG1-expressing cells responded to BCR cross-linking by normal or dampened—rather than enhanced—total tyrosine phosphorylation and c-Jun N-terminal kinase (JNK), extracellular signal–related kinase (ERK), Akt, nuclear factor of activated T cells 2, and IκBα phosphorylation (Fig. 4 B and not depicted), a clear difference between IgG1-expressing and WT cells in the stimulation experiments was enhanced Ca^{2+} mobilization upon BCR cross-linking (Fig. 4 C and Fig. S2, available at http://www.jem.org/cgi/content/full/jem.20062024/DC1). This enhanced response was also seen in mature B cells that had been acutely switched from IgM to IgG1 expression in vivo through induced Cre-mediated recombination (Fig. 4 E). The enhanced Ca^{2+} response in IgG1-expressing B cells is not caused by increased levels of BCR expression (Fig. S3). To address whether it results from an impairment of CD22 inhibition (7), $IgH^{\gamma1\mu/\gamma1\mu}$ mice were crossed to CD22 knockout animals, and anti-kappa–induced Ca^{2+} mobilization was measured in B cells from the compound mutants. Anti-kappa–induced Ca^{2+} signaling was strongly increased in $IgH^{\gamma1\mu/\gamma1\mu}$ $CD22^{-/-}$ B cells compared with the response of $IgH^{\gamma1\mu/\gamma1\mu}$ B cells, despite the fact that the latter is already considerably stronger than that of WT cells (Fig. 4 C). This increase in the Ca^{2+} response was found over a wide range of anti-kappa antibody concentrations (from 0.4 to 15 μg/ml; unpublished data). Thus, CD22 deficiency causes an increase of Ca^{2+} flux, irrespective of whether the cells express an IgM and IgD or an IgG1 BCR.

We also compared tyrosine phosphorylation of CD22 and Src homology domain 2–containing protein tyrosine phosphatase (SHP-1) recruitment between control (IgM/IgD-expressing) and IgG1-expressing B cells after BCR stimulation. Anti-kappa–stimulated splenic B cells were analyzed by immunoprecipitation of CD22, and equal tyrosine phosphorylation of CD22 was found in splenic B cells of control $IgH^{\gamma1\mu/\gamma1\mu}$ mice. We also could not detect any quantitative differences in SHP-1 recruitment to CD22 in the two types of cells when several experiments were quantified (Fig. 4 D). This is in contrast to the published results from cell line studies in which IgG2a B cells did not show any CD22 tyrosine phosphorylation and SHP-1 recruitment after stimulation with antigen (7). In that report, it was also postulated that there may be diminished association of CD22 to BCRs of the IgG2a isotype. Therefore, we performed immunoprecipitation with Igκ-specific antibodies and looked for the amount of coprecipitated CD22. We found that the same amount of CD22 protein could be coprecipitated from unstimulated and stimulated B cells of control and $IgH^{\gamma1\mu/\gamma1\mu}$ mice and that the coprecipitated CD22 exhibited comparable tyrosine phosphorylation (Fig. 4 D). We conclude that in IgG1-expressing B cells of $IgH^{\gamma1\mu/\gamma1\mu}$ mice, normal activation of CD22-dependent pathways takes place. The higher Ca^{2+} response of $IgH^{\gamma1\mu/\gamma1\mu}$ mice can also not be attributed to changed B cell subpopulations in their spleens, because a similarly increased Ca^{2+} response was detected in lymph-node B cells (Fig. S2).

We also addressed the question of whether CD22 deficiency affects B cell subsets in $IgH^{\gamma1\mu/\gamma1\mu}$ mice. In the BM, a similar composition of B cells was found in $IgH^{\gamma1\mu/\gamma1\mu}$ $CD22^{-/-}$ and $IgH^{\gamma1\mu/\gamma1\mu}$ mice. Although $CD22^{-/-}$ mice show a characteristic reduction of mature recirculating B cells ($B220^{hi}$ IgM^{+}), a reduction of $B220^{hi}$ $IgG1^{+}$ cells was not seen in $IgH^{\gamma1\mu/\gamma1\mu}$ mice on a CD22-deficient background (Fig. S4 A, available at http://www.jem.org/cgi/content/full/jem.20062024/DC1). In the spleen, a considerably higher number of $IgG1^{+}$ B cells was present in heterozygous $IgH^{\gamma1\mu/+}$,

(control), 1, 1.5 ± 0.8, 1.2 ± 0.8, and 1 ± 0; and $IgH^{\gamma1\mu/\gamma1\mu}$ mice, 1 ± 0.4, 1.4 ± 0.7, 1.2 ± 0.4, and 0.9 ± 0.3. To analyze CD22 association with the BCR, Igκ was immunoprecipitated from whole-cell lysates of splenic B cells. Coprecipitation of phosphorylated and total CD22 was determined by immunoblotting. Numbers at the bottom of each panel indicate fold increases of coprecipitated phosphorylated CD22 or coprecipitated total CD22 compared with unstimulated WT samples, normalized to anti-kappa signal. Means and SDs were calculated from three experiments in the same order as in the figure: anti-p-Tyr (control), 1, 1.3 ± 0.3, and 1.4 ± 0.5; $IgH^{\gamma1\mu/\gamma1\mu}$ mice, 10 ± 0.2, 1.3 ± 0.5, and 1.7 ± 1; total CD22 (control), 1, 1.1 ± 0.1, and 1 ± 0.1; and $IgH^{\gamma1\mu/\gamma1\mu}$ mice, 0.9 ± 0.1, 1.1 ± 0.2, and 1.1 ± 0.1. (E) Ca^{2+} mobilization upon BCR cross-linking in splenic B cells carrying the $IgH^{\mu\gamma1}$ allele, which were acutely switched to IgG1 orientation. Purified splenic B cells from $IgH^{\mu\gamma1/JHT}$ Cre-ER^{T2} mice treated with tamoxifen were stained with Cy5-conjugated anti-IgM Fab fragments and loaded with Fluo-3 and Fura Red. Loaded cells were gated for IgM^{+} or IgM^{-} (switched) and stimulated with the indicated doses of anti-kappa at the time points indicated by the arrows. The relative intracellular Ca^{2+} concentration is displayed as the ratio between Fluo-3 and Fura Red mean fluorescence intensity over time.

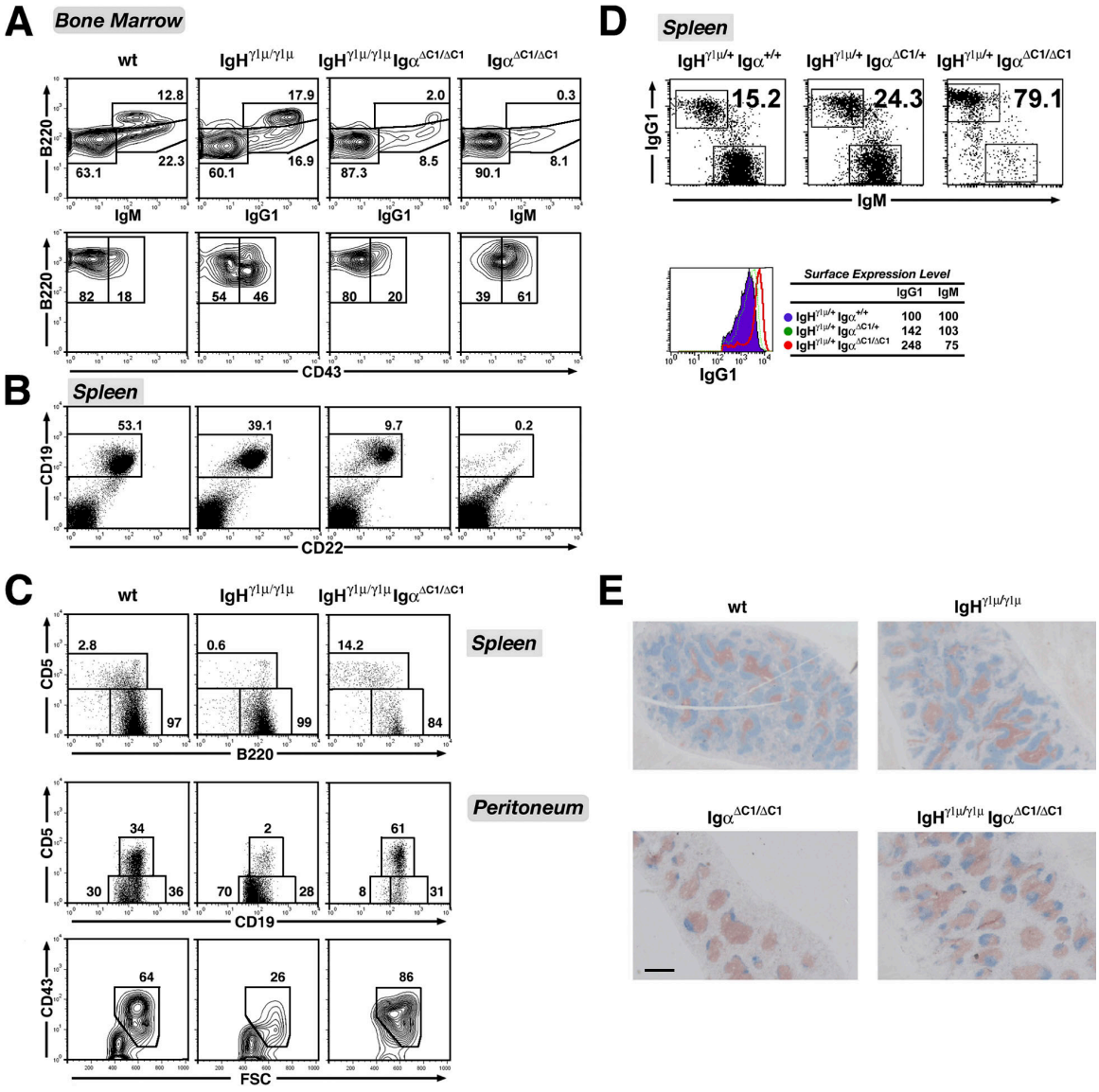

Figure 5. IgH$^{\gamma1\mu}$ B cells are less dependent on the Igα cytoplasmic domain than WT B cells. Flow cytometric analysis of compound mutant animals with the IgH$^{\gamma1\mu}$ and Igα$^{\Delta c1}$ alleles. (A) BM B220^{+} B cell subsets from mice with the indicated genotypes to determine the fractions of recirculating (B220^{high}Ig^{+}; fraction F) and immature (B220^{low}Ig^{+}; fraction E) B cells. (bottom) B220^{+}Ig^{-} BM cells were gated based on CD43 expression of pro- (CD43^{+}; fractions A–C) and pre-B cells (CD43^{-}; fraction D). (B) Splenic lymphocytes were stained for CD19 and CD22 expression. Note that CD22 expression levels are comparable for B cells from WT and IgH$^{\gamma1\mu/\gamma1\mu}$ mice. (C) Splenic (top) and peritoneal (middle) CD19^{+} B cells were analyzed for CD5 surface expression. (bottom) The size and CD43 expression levels of peritoneal CD19^{+} cells. (D, top) CD19^{+} splenic B cells from heterozygous IgH$^{\gamma1\mu}$ mice with the Igα mutation were analyzed for the expression of IgM and IgG1. (bottom) Relative surface expression levels (percentages) of IgG1 and IgM for CD19^{+} splenic B cells. Expression levels in the context of WT Igα are set to 100. The histogram shows a representative example. Numbers in A–D indicate the percentage of cells within the designated gates. (E) Spleen sections stained by immunohistochemistry to identify B cells (blue) and T cells (red). Bar, 1 mm.

CD22-deficient mice compared with their CD22-proficient counterparts (Fig. S4 B). The MZ B cell compartment was enlarged in both CD22-proficient and -deficient IgH$^{\gamma1\mu/\gamma1\mu}$ mice, contrasting the reduction of MZ B cells in CD22-deficient mice carrying WT IgH loci (however, note that differences in genetic backgrounds may play a role in this case; Fig. S4 C) (23). Similar to IgH$^{\gamma1\mu/\gamma1\mu}$ mice, IgH$^{\gamma1\mu/\gamma1\mu}$ CD22$^{-/-}$ mice had a strongly reduced B1a cell population in the peritoneal cavity (Fig. S4 D).

B cell development and maintenance in IgH$^{\gamma1\mu}$ mice is less dependent on an intact Igα/β heterodimer than in WT mice

Normal B cell development is severely compromised in mice carrying a mutation in the *mb-1* gene that leads to a partial

ablation of the cytoplasmic tail of the Igα signal transducer. Such animals generate <1% of normal mature B cell numbers, and these cells do not accumulate, presumably because of a shortened life span (24, 25). We wondered whether expression of the γ1 chain in the BCR would rescue B cell development and maintenance in mice carrying a truncated Igα chain. Therefore, double-mutant mice homozygous for the Igα truncation mutation ($Ig\alpha^{\Delta c1}$) and homo- or heterozygous for $IgH^{\gamma1\mu}$ were generated. The Igα truncation clearly impeded B cell development in the $IgH^{\gamma1\mu}$ mice, as reflected by reduced fractions of immature and mature B cells in the BM and spleen (Fig. 5, A and B; and Tables I and II). Like in WT mice, an Igα-null mutation led to a complete block of B cell development in $IgH^{\gamma1\mu/\gamma1\mu}$ mice (Fig. S5, available at http://www.jem.org/cgi/content/full/jem.20062024/DC1). However, in comparison to mice carrying the Igα truncation on a WT background, $Ig\alpha^{\Delta c1/\Delta c1}$ $IgH^{\gamma1\mu/\gamma1\mu}$ double mutants displayed a 10-fold larger fraction of mature B cells in the spleen (Fig. 5 B and Table II), which were partly organized into small B cell follicles (Fig. 5 E) and had a life span indistinguishable from that of their Igα-sufficient counterparts (Fig. 2 B). In accord with these results, when the Igα mutation was combined with $IgH^{\gamma1\mu/+}$ heterozygosity, we observed a dramatic preponderance of cells expressing IgG1 BCRs over those expressing BCRs associated with IgM (Fig. 5 D). We conclude that the presence of γ1 chains in the BCR makes the maintenance, but not the development, of the cells independent of the Igα cytoplasmic tail.

Curiously, combining the $IgH^{\gamma1\mu}$ with the $Ig\alpha^{\Delta c1}$ mutation promoted B1a cell development in both the peritoneal cavity and spleen beyond what is seen in $IgH^{\gamma1\mu/\gamma1\mu}$ mice (Fig. 5 C and Tables II and III). The fraction of these cells was strongly reduced in $IgH^{\gamma1\mu}$ mice, but when the majority of the B2 cells were depleted through the Igα mutation, they became the dominant fraction in the peritoneal cavity. We also noted that the splenic B cells developing in the double-mutant mice had increased surface levels of IgG1 BCRs, with some increase being detectable even in animals heterozygous for the Igα truncation (Fig. 5 D). However, the levels of BAFF-R on these cells were unaffected by the Igα truncation (unpublished data).

DISCUSSION

We describe a mouse strain whose IgH locus is engineered such that either membrane-bound γ1 or μ chains can be produced through Cre-mediated inversion of a loxP-flanked C_H region gene minilocus containing the Cγ1 and Cμ gene segments in opposite orientation. This strain can be used either for switching B cells from IgM to IgG1 expression, and vice versa, through induced Cre recombinase expression or to generate strains in which B cell development relies on the exclusive usage of membrane-bound μ or γ1 chains, respectively. In this paper, we use this system to study B cell development and maintenance in the latter situation. A main advantage of the present approach over earlier experiments, in which the developmental potential of IgH transgenes encoding H chains of various isotypes was analyzed, is that we can study B cell development under conditions in which the cells go through V_H region diversification, like in WT mice, instead of starting from a prerearranged IgH transgene encoding a single V_H region. We have indeed observed that homozygous $IgH^{\gamma1\mu}$ mice produce a highly diverse repertoire of IgH chain–variable regions in their mature B cell compartment, indistinguishable in a first approximation from that of WT mice (unpublished data). The present system also avoids the serious complications of copy number and position-dependent variations of transgene expression (15), in that IgH expression is controlled by the very same V_H promoters that are used in normal B cell development.

In homozygous $IgH^{\gamma1\mu}$ mice, all B cells indeed express IgG1, and in the blood of the animals we detect IgG1 but no IgM antibodies. Although B cells of all subsets are generated and the overall size of the peripheral B cell compartment is similar to the one for WT mice, B cell development in the BM is clearly compromised, with a partial developmental block at the pro– to pre–B cell transition. The nature of this block, whose elucidation will require the generation and analysis of pro–B cell lines from the mutant animals, likely lies in the inadequate assembly or signaling capacity of the pre-BCR (pBCR) in the mutant animals, given that the pBCR plays a crucial role at this very point in development (26, 27). Indeed, in pBCR-deficient mice, B cell development is largely blocked at the pro– to pre–B cell transition, at which the cells go through a pBCR-dependent phase of rapid proliferation. The developmental block seen in the $IgH^{\gamma1\mu}$ animals is clearly much milder, in that not only do many more B cells develop in these animals over time but also a normal fraction of large, cycling cells is seen in the pre–B cell compartment (unpublished data), which are lacking in pBCR-deficient mice (28). We therefore speculate that a γ1 chain–containing pBCR-like molecular complex is assembled in the animals but is functionally compromised. This problem is currently under investigation.

As predicted by this scenario, the mutant cells compete poorly in development with their WT counterparts in heterozygous $IgH^{\gamma1\mu}$ mice. This effect is more dramatic at the level of immature B cells in the BM and transitional T1 B cells in the spleen than that of mature splenic B cells. The accumulation of IgG1-expressing mature B cells in these animals could be explained by prolonged average life spans for these cells as compared with those of WT, IgM-, and IgD-expressing cells. At face value, this is indeed independently suggested by the BrdU chase data in Fig. 2 B, but one should bear in mind that these data could mainly reflect the dependence of B cell turnover on B cell output from the BM. It is well established that the average half-life of B cells is dramatically prolonged when B cell generation in the BM is blocked (29).

Homozygous $IgH^{\gamma1\mu/\gamma1\mu}$ mice showed characteristic shifts in peripheral B cell populations, with reduced numbers of B1 cells and higher splenic MZ B cell counts. Interestingly, a companion study by Horikawa et al. using transgenic mice that express a μ/γ1 transgenic BCR also found an increased

MZ B cell population (see Horikawa et. al [30] on p. 759 of this issue). Although the MZ B cell expansion may be related to a decreased cellular output from the BM, the B1 cell defect is likely caused by improper signaling properties of the IgG1 BCR. Our biochemical data from splenic B cells argue that these are not based on an uncoupling of the inhibitory CD22 receptor from the BCR. The B1 cell defect is likely also CD22 independent, because CD22 has been shown not to modulate the Ca^{2+} responses of B1 cells (31).

Mature B cells expressing an IgG1 BCR exhibited enhanced Ca^{2+} mobilization upon BCR cross-linking as compared with WT B cells, irrespective of whether the cells had gone through development as γ1-expressing cells or had their BCR switched from IgM to IgG1 after maturation. Although the biochemical basis of this enhanced signaling capacity of the IgG1 BCR remains to be elucidated, it clearly does not reflect an inability of the inhibitory CD22 receptor to dampen the response of the mutant cells, as earlier work on B cell lines expressing an IgG2a BCR had indirectly suggested (7). This is also born out in the accompanying study by Horikawa et al. (30) in which antigen-specific IgG1- and IgM-transgenic mice are compared with respect to their BCR responses and the role of CD22 inhibition. In the work of Wakabayashi et al. (7), an antigen-specific γ2a chain was stably expressed in various B cell lines. It is therefore possible that the results obtained in that study reflect a peculiarity of the particular IgH chain used or of the B cell clones selected. In the present system, as well as in that of Horikawa et al. (30), mice are used that express a diverse repertoire of γ1 chains in the B cell compartment in vivo. As γ2a and γ1 chains are very similar and no different functions have as yet been attributed to their cytoplasmic tails (32), we speculate that the present results may reflect common signaling properties of IgG BCRs in normal physiology.

Although the enhanced Ca^{2+} response to BCR cross-linking in B cells expressing IgG1 BCRs may reflect the unique signaling properties of the latter, we have so far been unable to identify signaling cascades that are selectively activated through the BCR in IgG1-expressing cells. Indeed, phophorylation of known players in BCR signaling like JNK, ERK, Akt, nuclear factor of activated T cells 2, and IκBα was normal or dampened, rather than enhanced, in these cells compared with their IgM- and IgD-expressing counterparts. Total tyrosine phosphorylation was also not enhanced in IgG1 cells. These issues clearly need further investigation, particularly in cells acutely switched from IgM to IgG1 expression.

We did not observe enhanced proliferation of the mutant cells upon TLR ligation in vitro, but upon BCR cross-linking, the fraction of highly proliferating cells was increased. The latter effect is likely not caused by an increased fraction of MZ B cells in the mutant mice, because follicular B cells proliferate better than MZ B cells upon BCR cross-linking (33). Our results are in line with earlier experiments by Martin and Goodnow (6) in which B cells expressing a transgenic IgG1 of defined antigenic specificity were triggered by antigen. The mutant cells in the latter study generated strikingly larger numbers of progeny cells than antigen- activated cells expressing transgenic IgM and IgD because of their enhanced survival. In the present experiments, the enhanced in vitro proliferation upon BCR cross-linking, as well as the accumulation of IgG1-expressing cells in the mature B cell compartment in the heterozygous mutant animals (i.e., when the cells compete with IgM- and IgD-expressing cells), may similarly reflect an enhanced efficiency by which survival signals are delivered to the cells via the BCR upon isotype switching, as it typically occurs in the generation of memory B cells. It will be interesting to see whether we can use the present experimental system to bestow enhanced in vivo survival to IgM-expressing cells by switching them to IgG1 expression through induced Cre recombinase activity and, thus, to assess whether expression of the IgG1 BCR as such increases the life span of these cells.

As the BCR acquires a new signaling module in terms of the cytoplasmic tail and, perhaps, other parts of the newly expressed IgH chain upon isotype switching, it was of interest to ask whether the cytoplasmic tails of the Igα/β heterodimer, which mediate signal transduction through IgM and IgD BCRs, are required for the maintenance of B cells expressing an IgG1 BCR. Indeed, we had previously shown that the Igα cytoplasmic tail is required for the survival of mature B cells in WT mice (24, 25). We now demonstrate that, in contrast to this result, the partial truncation of the Igα cytoplasmic tail does not impede the survival of B cells expressing an IgG1 BCR. The simplest interpretation of this finding is that, in accord with the considerations above, the γ1 chain, likely through its conserved cytoplasmic tail, indeed delivers a survival signal to the cells, and that this signal contributes to the longevity of memory B cells expressing class-switched BCRs. However, we also note that in the compound mutant animals, B cell development is profoundly compromised, in that the animals produce only one tenth of the normal numbers of B cells. Although this is still roughly 10 times more cells than in animals carrying a WT IgH locus in combination with the Igα truncation (24, 25), we cannot exclude that the cells generated in these animals are a selected population of B cells that are not representative of the B cell population generated in WT mice.

MATERIALS AND METHODS

Mice. $Ig\alpha^{\Delta C1/\Delta C1}$, $Ig\alpha^{\Delta Tm/\Delta Tm}$, BAFF-$R^{-/-}$, and $CD22^{-/-}$ mice were described previously (24, 34, 35) and kept on C57BL/6 ($Ig\alpha^{\Delta Tm/\Delta Tm}$ and BAFF-$R^{-/-}$), 129 ($CD22^{-/-}$), or mixed 129 × C57BL/6 ($Ig\alpha^{\Delta C1/\Delta C1}$) genetic backgrounds. Mice were analyzed at the ages of 6–16 wk. The generation of the $IgH^{\mu\gamma1}$ and $IgH^{\gamma1\mu}$ mouse strains is described in Fig. S1. Both strains were generated from BALB/c-derived ES cells and kept on a BALB/c background. The sequence of the mutant locus is available from GenBank/EMBL/DDBJ under accession no. EF495199. Mice were bred and maintained under specific pathogen-free conditions. Animal care and experiments were conducted according to protocols approved by the Harvard University Institutional Animal Care and Use Committee and by the CBR Institute for Biomedical Research.

Flow cytometry. Preparations of cell suspensions from lymphoid organs and cell-surface stainings were performed as previously described (36). Data were acquired on a FACSCalibur (BD Biosciences) and analyzed using CellQuest

(BD Biosciences) and FlowJo (TreeStar Inc.) software. Dead cells were labeled with propidium iodide or TO-PRO-3 iodide (Invitrogen) and excluded from the analysis. Monoclonal antibodies R33-24.12 (anti-IgM), 1.3-5 (anti-IgD), RA3-6B2 (anti-B220), R33-18-10 (anti-Igκ), and M5/114 (anti-IA^b) were prepared and conjugated in our laboratory. Monoclonal antibodies to CD5, CD19, CD21/35, CD22, CD23, CD24, CD25, CD43, CD69, CD86, CD95, CD117, Igλ, IgG1, and H2Kb were purchased from BD Biosciences. The monoclonal antibody to AA4.1 was purchased from eBioscience. AA4.1-PE (anti-$C1qR_p$) was a gift from M.P. Cancro (University of Pennsylvania School of Medicine, Philadelphia, PA). Rabbit polyclonal antibodies to mouse BAFF-R were generated as previously described (34). Ig serum concentrations were determined by ELISA, as described previously (36).

BrdU labeling and block of B cell lymphopoiesis. 0.8 mg/ml BrdU (Sigma-Aldrich) was given in the drinking water for 31 d. Lymphocytes were surface stained for CD19 and CD21, and BrdU incorporation was determined with the BrdU Flow Kit (BD Biosciences).

To block B cell lymphopoiesis in the BM of $IgH^{g1m/+}$ heterozygous mice, 1 mg anti–IL-7R monoclonal antibody (A7R34) was injected i.v. every second day.

B cell activation. 2–10 × 10^6 B cells/ml were incubated with carboxyfluorescein succinimidyl ester (CFSE; Invitrogen) in RPMI 1640 (Invitrogen) containing 5 mM CFSE for 5 min at 37°C. CFSE-labeled cells were cultured in 200 μl complete DMEM (Invitrogen) at a concentration of 4 × 10^6 cells/ml in 96-well microtiter plates at 37°C in the presence of different mitogenes. Cells were analyzed by flow cytometry. For activation, anti-RP105 antibody (eBioscience), LPS (*Salmonella minnesota* Re 595; Sigma-Aldrich), IL-4 (PeproTech), anti-CD40 (BD Biosciences), CpG (phosphothioate-stabilized CpG-ODN [TCCATGACGTTCCTGATGCT]; TIB MOLBIOL), or anti-IgM $F(ab')_2$ fragments (Jackson Immuno Research Laboratories) or anti-kappa (Southern Biotechnology Associates, Inc.) were used.

Ca^{2+} mobilization. Splenocytes were resuspended in RPMI 1640 supplemented with 1% FCS (5 × 10^6 cells/ml) and incubated with 4.5 μM Indo-1 and 0.003% Pluronic F-127 (Invitrogen) at 37°C for 45 min. Afterward, splenocytes were stained on ice with anti–Mac-1–FITC and anti-CD5–PE (BD Biosciences), followed by acquisition with a FACSVantage (BD Biosciences) and stimulation with anti-kappa at the concentrations indicated in Fig. 4. Data were analyzed using FlowJo software.

Immunoblotting and immunoprecipitation. After red blood lysis, splenic B cells were negatively selected using CD43 magnetic beads (Miltenyi Biotec) and stained with B220, CD21, and CD23 antibodies. Follicular B cells ($B220^+$, $CD21^+$, $CD23^{bright}$) were sorted with a FACSVantage and resuspended in complete B cell medium at a concentration of 2 × 10^6 cells/ml. After preincubation for 1 h at 37°C, cells were stimulated with 20 μg/ml anti-kappa and lysed in RIPA lysis buffer (40 mM Tris, pH 7.6, 150 mM NaCl, 2 mM EDTA, 1% NP-40, 0.25% sodium deoxycholate, 5 μg/ml aprotinin, 2 μM pepstatin, 10 μg/ml leupeptin, 1 mM PMSF, 5 mM NaF, 0.5 μM okadaic acid, 1 mM Na_3VO_4). Protein concentrations were determined by a Protein Assay Kit (Bio-Rad Laboratories), and 6 μg of protein per lane was separated by a 10% SDS-PAGE and transferred to a polyvinylidene difluoride membrane (Millipore). The membranes were immunoblotted with phospho-ERK1/2 (T202/Y204), phospho-JNK1/2 (T183/Y185), phospho-Akt (S473), phospho-IκBα (S32/36), anti-ERK1/2, anti-JNK1/2, anti-Akt (Cell Signaling), anti-IκBα (Santa Cruz Biotechnology, Inc.), and anti–β-actin (Sigma-Aldrich) antibodies.

For co-immunoprecepitation experiments, splenic B cells were purified after erythrocyte lysis by a complement lysis of T cells. 10^7 B cells/ml were stimulated with anti-kappa at 37°C for the times indicated in the figures. After stimulation, cells were lysed in lysis buffer (50 mM Tris [Roth], pH 7.5, 6.6 mM NaCl [Roth], 0.5 mM EDTA [Applichem], 1 μg/ml aprotonin [Roche], 5 μg/ml leupeptin [Roche], 1 mM PMSF [Roche], 1 mM Na_3VO_4 [Sigma-Aldrich], 1% Brij-58 [Sigma-Aldrich]) and incubated for 30 min on ice. The lysates were centrifuged and immunoprecipitated with rabbit anti-CD22 (a gift from P. Crocker, University of Dundee, Dundee, UK) and protein A–sepharose (GE Healthcare) or anti-kappa antibody and protein G–sepharose (GE Healthcare). Immune-complexed coated beads were collected after overnight incubation and washed three times with ice-cold lysis buffer. After boiling the beads for 3 min in a reducing sample buffer, supernatants were separated by a 7.5% SDS-PAGE and transferred to nitrocellulose membranes (BioTrace NT; Pall). Membranes were incubated with primary antibodies 4G10 (Upstate Biotechnology), SHP-1 (Biozol), and anti-kappa overnight at 4°C. Secondary antibodies were goat anti–mouse IgG–horseradish peroxidase (HRP; Jackson ImmunoResearch Laboratories) and goat anti–rabbit IgG-HRP (Santa Cruz Biotechnology, Inc.). Membranes were developed with ECL (GE Healthcare). Blots were scanned, and band intensities were quantified using ImageJ software (National Institutes of Health).

In vivo induction of IgG1 expression and Ca^{2+} flux measurement in switched cells. To induce in vivo inversion of the $IgH^{\mu\gamma1}$ allele with subsequent expression of IgG1 instead of IgM in B cells, $IgH^{\mu\gamma1/JHT}$ Cre-ER^{T2} (37) mice were fed for 3 d with 1–5 mg tamoxifen (Sigma-Aldrich) per mouse by gavage (depending on the weight of the recipients). 3 d after discontinuation of tamoxifen, splenocytes from treated mice were harvested, and B cells were negatively selected using CD43-MACS beads (Miltenyi Biotec). After purification, cells were stained with Cy5-conjugated anti-IgM Fab fragments, washed twice, and labeled with Fluo-3 and Fura Red (Invitrogen). Ca^{2+} flux of B cells resuspended at 2 × 10^6 cells/ml in Krebs-Ringer solution (1 mM Ca^{2+}) was assayed by flow cytometry (FACSCalibur), measuring the fluorescence emission of Fluo-3 in the FL-1 channel and Fura Red in the FL-3 channel. Data were analyzed using FlowJo software.

Immunohistochemistry. For histological staining of B cells and T cells, frozen 6-μm sections were thawed, air dried, fixed in acetone, and stained for 1 h at room temperature in a humidified chamber with rat anti-CD19 (ID3; BD Biosciences) and biotinylated anti-CD3 (145-2C11; BD Biosciences), followed by HRP-conjugated goat anti–rat IgG and alkaline phosphatase–conjugated streptavidin (Southern Biotechnology Associates, Inc.).

Online supplemental material. Fig. S1 shows the targeting strategy to generate $IgH^{\gamma1\mu}$ or $IgH^{\mu\gamma1}$ alleles. Fig. S2 and Fig. S3 demonstrate enhanced Ca^{2+} responses in lymph-node B cells of $IgH^{\gamma1\mu/\gamma1\mu}$ mice or acutely switched splenic B cells, respectively. Fig. S4 shows that CD22 deficiency does not affect B cell development in $IgH^{\gamma1\mu/\gamma1\mu}$ mice but results in accumulation of a higher number of $IgG1^+$ cells in heterozygous mice. Fig. S5 demonstrates that $IgG1^+$ B cells do not develop in the absence of Igα. Online supplemental material is available at http://www.jem.org/cgi/content/full/jem.20062024/DC1.

We thank Kevin Otipoby and Gunther Galler for discussions, Christine Patterson for critical reading of the manuscript, Claudia Uthoff-Hachenberg, Angela Egert, Christian Linden, and Jing Wang for excellent technical help, and John P. Manis for help with planning the targeting construct and probes.

This work was supported by the FP6 Marie Curie Research Training Network (grant MRTN-CT-2004-005632 to A. Waisman), the Deutsche Forschungsgemeinschaft (grant SFB 243 to K. Rajewsly, grant SFB 490 to A. Waisman, and grant SFB 466 to L. Nitschke), and the National Institutes of Health (grant 1 R37 AI054636-01). J. Seagal was supported by a Dorot fellowship and a fellowship from the Cancer Research Institute, J. Song was supported by the Center for Molecular Medicine Cologne, Y. Sasaki was supported by the Uehara Memorial Foundation, and D. Melamed was supported by a fellowship from the International Union Against Cancer.

The authors have no conflicting financial interests.

Submitted: 20 September 2006
Accepted: 1 March 2007

REFERENCES

1. Reth, M. 1994. B cell antigen receptors. *Curr. Opin. Immunol.* 6:3–8.
2. Geisberger, R., R. Crameri, and G. Achatz. 2003. Models of signal transduction through the B-cell antigen receptor. *Immunology*. 110:401–410.
3. Neuberger, M.S., H.M. Caskey, S. Pettersson, G.T. Williams, and M.A. Surani. 1989. Isotype exclusion and transgene down-regulation in immunoglobulin-lambda transgenic mice. *Nature*. 338:350–352.
4. Achatz, G., L. Nitschke, and M.C. Lamers. 1997. Effect of transmembrane and cytoplasmic domains of IgE on the IgE response. *Science*. 276:409–411.
5. Kaisho, T., F. Schwenk, and K. Rajewsky. 1997. The roles of gamma 1 heavy chain membrane expression and cytoplasmic tail in IgG1 responses. *Science*. 276:412–415.
6. Martin, S.W., and C.C. Goodnow. 2002. Burst-enhancing role of the IgG membrane tail as a molecular determinant of memory. *Nat. Immunol.* 3:182–188.
7. Wakabayashi, C., T. Adachi, J. Wienands, and T. Tsubata. 2002. A distinct signaling pathway used by the IgG-containing B cell antigen receptor. *Science*. 298:2392–2395.
8. Roes, J., and K. Rajewsky. 1991. Cell autonomous expression of IgD is not essential for the maturation of conventional B cells. *Int. Immunol.* 3:1367–1371.
9. Lutz, C., B. Ledermann, M.H. Kosco-Vilbois, A.F. Ochsenbein, R.M. Zinkernagel, G. Kohler, and F. Brombacher. 1998. IgD can largely substitute for loss of IgM function in B cells. *Nature*. 393:797–801.
10. Roth, P.E., B. Kurtz, D. Lo, and U. Storb. 1995. λ5, but not μ, is required for B cell maturation in a unique γ2b transgenic mouse line. *J. Exp. Med.* 181:1059–1070.
11. Roth, P.E., L. Doglio, J.T. Manz, J.Y. Kim, D. Lo, and U. Storb. 1993. Immunoglobulin γ2b transgenes inhibit heavy chain gene rearrangement, but cannot promote B cell development. *J. Exp. Med.* 178:2007–2021.
12. Yamamura, K., A. Kudo, T. Ebihara, K. Kamino, K. Araki, Y. Kumahara, and T. Watanabe. 1986. Cell-type-specific and regulated expression of a human gamma 1 heavy-chain immunoglobulin gene in transgenic mice. *Proc. Natl. Acad. Sci. USA*. 83:2152–2156.
13. Battegay, M., P. Fiedler, U. Kalinke, F. Brombacher, R.M. Zinkernagel, H.H. Peter, G. Kohler, and H. Eibel. 1996. Non-tolerant B cells cause autoimmunity in anti-CD8 IgG2a-transgenic mice. *Eur. J. Immunol.* 26:250–258.
14. Offen, D., L. Spatz, H. Escowitz, S. Factor, and B. Diamond. 1992. Induction of tolerance to an IgG autoantibody. *Proc. Natl. Acad. Sci. USA*. 89:8332–8336.
15. Pogue, S.L., and C.C. Goodnow. 2000. Gene dose-dependent maturation and receptor editing of B cells expressing immunoglobulin (Ig)G1 or IgM/IgG1 tail antigen receptors. *J. Exp. Med.* 191:1031–1044.
16. Roark, J.H., C.L. Kuntz, K.A. Nguyen, L. Mandik, M. Cattermole, and J. Erikson. 1995. B cell selection and allelic exclusion of an anti-DNA Ig transgene in MRL-lpr/lpr mice. *J. Immunol.* 154:4444–4455.
17. Iliev, A., L. Spatz, S. Ray, and B. Diamond. 1994. Lack of allelic exclusion permits autoreactive B cells to escape deletion. *J. Immunol.* 153:3551–3556.
18. Bynoe, M.S., L. Spatz, and B. Diamond. 1999. Characterization of anti-DNA B cells that escape negative selection. *Eur. J. Immunol.* 29:1304–1313.
19. Tsao, B.P., K. Ohnishi, H. Cheroutre, B. Mitchell, M. Teitell, P. Mixter, M. Kronenberg, and B.H. Hahn. 1992. Failed self-tolerance and autoimmunity in IgG anti-DNA transgenic mice. *J. Immunol.* 149:350–358.
20. Chu, Y.P., L. Spatz, and B. Diamond. 2004. A second heavy chain permits survival of high affinity autoreactive B cells. *Autoimmunity*. 37:27–32.
21. Sudo, T., S. Nishikawa, N. Ohno, N. Akiyama, M. Tamakoshi, and H. Yoshida. 1993. Expression and function of the interleukin 7 receptor in murine lymphocytes. *Proc. Natl. Acad. Sci. USA*. 90:9125–9129.
22. Smith, S.H., and M.P. Cancro. 2003. Cutting edge: B cell receptor signals regulate BLyS receptor levels in mature B cells and their immediate progenitors. *J. Immunol.* 170:5820–5823.
23. Samardzic, T., D. Marinkovic, C.P. Danzer, J. Gerlach, L. Nitschke, and T. Wirth. 2002. Reduction of marginal zone B cells in CD22-deficient mice. *Eur. J. Immunol.* 32:561–567.
24. Kraus, M., M.B. Alimzhanov, N. Rajewsky, and K. Rajewsky. 2004. Survival of resting mature B lymphocytes depends on BCR signaling via the Igalpha/beta heterodimer. *Cell*. 117:787–800.
25. Torres, R.M., H. Flaswinkel, M. Reth, and K. Rajewsky. 1996. Aberrant B cell development and immune response in mice with a compromised BCR complex. *Science*. 272:1804–1808.
26. Rolink, A.G., C. Schaniel, M. Busslinger, S.L. Nutt, and F. Melchers. 2000. Fidelity and infidelity in commitment to B-lymphocyte lineage development. *Immunol. Rev.* 175:104–111.
27. Martensson, I.L., A. Rolink, F. Melchers, C. Mundt, S. Licence, and T. Shimizu. 2002. The pre-B cell receptor and its role in proliferation and Ig heavy chain allelic exclusion. *Semin. Immunol.* 14:335–342.
28. Kitamura, D., A. Kudo, S. Schaal, W. Muller, F. Melchers, and K. Rajewsky. 1992. A critical role of lambda 5 protein in B cell development. *Cell*. 69:823–831.
29. Hao, Z., and K. Rajewsky. 2001. Homeostasis of peripheral B cells in the absence of B cell influx from the bone marrow. *J. Exp. Med.* 194:1151–1164.
30. Horikawa, K., S.W. Martin, S.L. Pogue, K. Peng, K. Takatsu, and C.C. Goodnow. 2007. Enhancement and suppression of signaling by the conserved tail of IgG memory–type B cell antigen receptors. *J. Exp. Med.* 204:759–769.
31. Lajaunias, F., L. Nitschke, T. Moll, E. Martinez-Soria, I. Semac, Y. Chicheportiche, R.M. Parkhouse, and S. Izui. 2002. Differentially regulated expression and function of CD22 in activated B-1 and B-2 lymphocytes. *J. Immunol.* 168:6078–6083.
32. Venkitaraman, A.R., G.T. Williams, P. Dariavach, and M.S. Neuberger. 1991. The B-cell antigen receptor of the five immunoglobulin classes. *Nature*. 352:777–781.
33. Oliver, A.M., F. Martin, G.L. Gartland, R.H. Carter, and J.F. Kearney. 1997. Marginal zone B cells exhibit unique activation, proliferative and immunoglobulin secretory responses. *Eur. J. Immunol.* 27:2366–2374.
34. Sasaki, Y., S. Casola, J.L. Kutok, K. Rajewsky, and M. Schmidt-Supprian. 2004. TNF family member B cell-activating factor (BAFF) receptor-dependent and -independent roles for BAFF in B cell physiology. *J. Immunol.* 173:2245–2252.
35. Nitschke, L., R. Carsetti, B. Ocker, G. Kohler, and M.C. Lamers. 1997. CD22 is a negative regulator of B-cell receptor signalling. *Curr. Biol.* 7:133–143.
36. Kraus, M., L.I. Pao, A. Reichlin, Y. Hu, B. Canono, J.C. Cambier, M.C. Nussenzweig, and K. Rajewsky. 2001. Interference with immunoglobulin (Ig)α immunoreceptor tyrosine–based activation motif (ITAM) phosphorylation modulates or blocks B cell development, depending on the availability of an Igβ cytoplasmic tail. *J. Exp. Med.* 194:455–469.
37. Seibler, J., B. Zevnik, B. Kuter-Luks, S. Andreas, H. Kern, T. Hennek, A. Rode, C. Heimann, N. Faust, G. Kauselmann, et al. 2003. Rapid generation of inducible mouse mutants. *Nucleic Acids Res.* 31:e12.
38. Hardy, R.R., C.E. Carmack, S.A. Shinton, J.D. Kemp, and K. Hayakawa. 1991. Resolution and characterization of pro-B and pre–pro-B cell stages in normal mouse bone marrow. *J. Exp. Med.* 173:1213–1225.